CORE
Metadata, citation and similar papers at core.ac.uk
Provided by NASA Technical Reports Server

NASA Technical Memorandum 102832

Microwave Landing System Modeling with Application to Air Traffic Control

M. M. Poulose

(NASA-TM-102832) MICROWAVE LANDING SYSTEM MODELING WITH APPLICATION TO AIR TRAFFIC CONTROL (NASA) 23 p CSCL 01C
N91-23099
Unclas
G3/03 0014951

April 1991

National Aeronautics and Space Administration

NASA Technical Memorandum 102832

Microwave Landing System Modeling with Application to Air Traffic Control

M. M. Poulose, Ames Research Center, Moffett Field, California

April 1991

National Aeronautics and
Space Administration

Ames Research Center
Moffett Field, California 94035-1000

SUMMARY

Compared to the current instrument landing system, the microwave landing system (MLS), which is in the advanced stage of implementation, can potentially provide significant fuel and time savings as well as more flexibility in approach and landing functions. However, the expanded coverage and increased accuracy requirements of the MLS make it more susceptible to the features of the site in which it is located. This report presents an analytical approach for evaluating the multipath effects of scatterers that are commonly found in airport environments. The approach combines a multiplate model with a ray-tracing technique and a formulation for estimating the electromagnetic fields caused by the antenna array in the presence of scatterers. It can model the effects of undulation, the roughness and impedance of the terrain, and other scatterers. The model is applied to several airport scenarios. The reduced computational burden enables the scattering effects on MLS position information to be evaluated in near-real time. Evaluation in near-real time would permit the incorporation of the modeling scheme into air traffic control automation; it would adaptively delineate zones of reduced accuracy within the MLS coverage volume, and help establish safe approach and takeoff trajectories in the presence of uneven terrain and other scatterers.

INTRODUCTION

Since an aircraft that is about to land has very low margins of speed and altitude to effect a recovery in case of loss of control, accuracy of guidance information is crucial to a safe and comfortable landing. The need for accuracy is becoming even greater as air traffic densities increase at terminal areas. The microwave landing system (MLS) was developed in response to the need for greater traffic handling capacity, accuracy and versatility of landing guidance, and reduced susceptibility to disturbing effects of site reflections (refs. 1–3). The MLS has gone through an extended period of development and proving and is at the beginning phase of operational installation. This system can be affected by certain kinds of interference, however, especially because of the dense traffic that it is expected to handle.

The effect of interference may be more critical on MLS than on the currently used instrument landing system (ILS). This is because the MLS is designed to provide multiple approach corridors to aircraft. There is thus less margin for error in the MLS than there is in the ILS, in which errors become catastrophic only when they are so large as to affect obstruction clearance. A second reason for the sensitivity of MLS is its higher operating frequency, which makes small scatterers appear electrically larger. Thus the effects of objects like parked or moving automobiles or aircraft, which are not significant at ILS frequencies, will be enhanced at MLS frequencies (ref. 4).

The experimental method used for MLS evaluation has important drawbacks. Setting up the equipment and performing the experiment is time-consuming and expensive. Another, perhaps more serious, limitation of the experimental method is that it provides information on MLS behavior for an existing site only "as is." If the site is not found suitable, the method cannot provide guidance regarding the nature and extent of site development necessary to make it acceptable.

Air traffic control (ATC) automation (refs. 5 and 6) is another area where insight into MLS behavior is crucial. Since MLS is designed to provide multiple approach corridors for aircraft, relatively small

aberrations could increase the probability of conflict among approaching aircraft. A priori knowledge about the course aberrations would enable appropriate margins to be built into the ATC automation tool.

There is thus a strong motivation for research into analytical methods for site evaluation, and, preferably, avoiding experimental procedures. Because of the availability of large computing power, such methods would be inexpensive, and they could predict MLS behavior for several assumed terrain shapes and scattering objects.

A model developed by Evans et al. (ref. 7) is based on the Fresnel–Kirchoff diffraction formula (refs. 8 and 9) which is integrated over a rectangular region. In this method, the ground surface is divided into triangular or rectangular plane surface elements, and the small-scale roughness is handled using the Beckmann–Spizzichino approximation (ref. 10). The Evans model mainly uses a combination of physical optics and geometric optics to obtain the desired accuracy with reasonable computation speed. However, in applying the physical optics method, the simplifying assumption is usually made that the ground currents in one area have no effect on those in neighbouring areas. Such an assumption is necessary to determine the fields within reasonable computation time, but it implies that the electric fields radiated by the ground pass through any subsequent obstructions as if they do not exist.

Another MLS model, developed by ITT Gilfillan (ref. 11), uses the geometric theory of diffraction to determine the fields. However, this model makes simplifying assumptions with regard to ray types and conductivity to keep the computation time within reasonable limits.

This report presents an analytical approach for determining the quality of MLS performance in the presence of non-ideal scatterers based on an impedance uniform theory of diffraction (impedance UTD) model and a closed-form geometric method for ray tracing. This modeling choice is expected to increase the modeling accuracy with far less evaluation time and expense, given the low cost and high accessibility of modern computing systems. The model is applied to terrain geometries and the results are compared with earlier results. Finally, the use of MLS scatter-effect modeling in ATC automation is discussed.

SYSTEM FEATURES

The time-reference scanning beam (TRSB) MLS system composition is shown in figure 1. It consists of forward azimuth, elevation, back azimuth, and flare equipment operating in the 5000-MHz carrier frequency band.

The MLS uses two narrow beams which are scanned in an oscillatory manner in the azimuth and elevation sectors. At every position within the scan sector, an aircraft will receive two pulses from each beam, which correspond to the to and fro scans. The aircraft derives its position within the coverage volume by measuring the time between these pulses, pairwise.

The azimuth scanner uses a fan beam that is broad in the vertical plane and narrow in the horizontal plane. Similarly, the elevation scanner moves up and down using a fan beam that is broad in the horizontal plane and narrow in the vertical plane. Each beam scans its assigned sector (azimuth or elevation) at a constant sweep rate. There is a final dwell time (time of transit of the beam during which

it exceeds the threshold level) at the end of each stroke. A schematic representation of beam sweep angle as a function of time is shown in figure 2. The same figure applies to both beams with different scales.

For a given scanning speed and pause time, the elevation (or azimuth) angle θ is calculated from the equation

$$\theta = (\Delta t_o - \Delta t)\omega/2$$

where

ω scan rate of the beam (0.02° per microsecond)

Δt actual time interval between pulses received from to and fro scans, in microseconds

Δt_o value of Δt in microseconds for θ = 0 (4800 μsec for azimuth and 3350 μsec for elevation).

MLS Multipath Effects

The MLS has a more elaborate design than the ILS; the objectives are to increase the traffic-handling capacity and reduce the site effects (ref. 12). The beam configuration makes it possible for the MLS to cover a much larger sector than the ILS, which has a narrow beam. Also, extensive effort has been put into the design of the radiation patterns of the MLS antennas to achieve a sharp cutoff at ground grazing angles (ref. 13). The sharp cutoff minimizes the power radiated in the direction of terrain features, resulting in reduced site effects.

The study of site effects is nevertheless important for the MLS. First, the standard terrain conditions assumed for the MLS may not be valid everywhere. For example, the lower scanning limit of 1° for the vertical scan is designed to ensure that the elevation coverage beam stays clear of the ground at its lowest position; this may not hold up if the ground has significant slope. Scattering due to sidelobes could also have a significant interfering effect (ref. 14).

The error arising from a multipath signal depends on its angular separation, δ, from the direct signal. The multipath signal at an angular coordinate different from the direct signal will result in the shifting of the centroids of the received beam shapes. Given the transmitter beamwidth, $\Delta\theta$, and the amplitude ratio, A_r, the in-beam multipath error when δ is less than 1.5 $\Delta\theta$ can be on the order of $A_r\Delta\theta/2$ (ref. 15). The out-of-beam multipath will be of concern only when its level remains high compared to the direct signal for a sufficiently long time. This duration can be typically 5 sec and the worst case error in such situations can be $A_r\Delta\theta$ times the sidelobe amplitude ratio.

THEORETICAL BACKGROUND

The electromagnetic energy sensed by an approaching aircraft is influenced by the presence of scattering objects between the transmitting antenna and that aircraft. Early efforts at evaluating electromagnetic fields in the presence of scatterers were based on physical optics (refs. 16 and 17). In physical optics, fields are evaluated from assumed currents through a process of integration. This method requires heavy computational effort, even by the standards of modern large computers, and it

cannot model obstructions and shadow effects. Since the scatterers and their significant features are large compared to the operating wavelength, the scattering behavior is expected to be close to optical in nature (ref. 18). This makes a ray-theoretic approach a natural choice, and such an approach has been used predominantly in recent studies (refs. 19 and 20). A simple model considers only the direct rays from the antenna array to the aircraft and the rays reaching the aircraft from the antenna after being once reflected from the scatterer. However, this model predicts discontinuous fields resulting from shadow effects. Such a prediction contradicts the physical reality that the electromagnetic fields in space are continuous.

Continuity of electromagnetic fields is ensured by including the effects of diffraction of the direct and reflected rays by the scatterers. The geometric theory of diffraction (GTD) (ref. 21), proposed by Keller in 1962, is based on such an approach. The GTD was a major improvement in the accuracy of prediction of scattering from complex surfaces. The theory predicts the electromagnetic field accurately nearly everywhere in the space surrounding a scatterer, except within a discrete number of narrow sections along reflection and shadow boundaries (fig. 3). Along these boundaries, the GTD exhibits singular behaviour, predicting infinite fields.

The field singularity problem has been solved, with modern uniform theories. Two well known theories of this class are the uniform theory of diffraction (UTD) (refs. 22 and 23) and the uniform asymptotic theory (ref. 24). These theories use different approaches for the determination of the diffraction coefficient, but each predicts a continuous and bounded field estimate.

The perfectly conducting model does not take into account the surface roughness and impedance properties of the scatterer. These properties have been taken into account in the impedance UTD formulation (ref. 25) in which the diffraction coefficient has been modified by introducing the Maliuzhinets function (ref. 26) (see appendix).

The beam envelope received by an aircraft consists of the superimposed patterns corresponding to the various signal paths. The model determines the angle by determining the point of zero derivative on the beam envelope in a manner analogous to what is done in the aircraft receiver.

MODELING

To study the effects of interference resulting from electromagnetic energy scattered by the terrain, it is necessary to model the characteristics of the terrain responsible for scattering. Both the shape and the electromagnetic characteristics of the surface need to be taken into account (ref. 27). The shape should ideally be described as a bivariate function that exactly specifies the height of each point on the terrain in terms of its horizontal (x-y) coordinates. However, such a description would make scattering computations difficult, hence a simpler description is desirable.

One simple and widely used model for studies of terrain effect is the multiplate or multiwedge model (refs. 28–30). In such a model (see fig. 4), the terrain is assumed to consist of a succession of flat plates. If adjacent pairs of plates are considered to constitute wedges, the model may also be viewed as consisting of a succession of straight-edged wedges. The model is so formed that the edges of the wedges are perpendicular to the extended runway center line.

The generation of a multiplate or multiwedge model for a particular airport is straightforward. The starting point is a contour map of the airport and the surrounding area, which is normally readily available. Drawing a line on the contour map from the MLS antenna parallel to the runway center line gives the terrain profile (fig. 4). This profile is then approximated by straight line segments. For mild undulations such as are found commonly at airport sites, fewer than 15 straight line segments will be adequate to fully describe the terrain effects; a larger number may be necessary for hilly areas. After the straight-segment profile line is formed, it is translated laterally, parallel to itself, to generate the multiwedge model of the terrain.

Other surface properties of the terrain that affect its scattering behavior are the impedance and roughness of the surface. In most locations the terrain surface impedance may be neglected, i.e., the surface assumed to be fully conducting. This is because normal soil with significant loam and moisture content has low surface impedance, and thus the original uniform theories are valid. However, in certain special locations, particularly those with dry and sandy soils, impedance effects cannot be neglected and must be built into the model. It is possible to incorporate terrain roughness effects into the model by using an equivalence relation that expresses the roughness in terms of an equivalent surface impedance which may be added to the inherent surface impedance (ref. 27). The multiwedge approximation, after incorporation of the surface impedance and roughness effects, constitutes the complete model of the terrain that is used to evaluate the site effects.

Objects like hangars and other buildings are modeled in a similar way, using the multiplate modeling approach. The multipath levels from aircraft surfaces such as the front and rear of the fuselage, leading and trailing edges of wings, and engines, are shown to be 15 dB lower than those of the fuselage (main body) and the tail fin (ref. 31). It is therefore assumed that the fuselage and the tail fin are the significant scatterers for MLS multipath effects, and they are considered in this work. For each aircraft position, a profile of the fuselage and tail fin is determined with respect to the antenna location for scattering computations.

RAY TRACING

The presence of multiple scatterers (wedges, in the model) means that the electromagnetic rays radiated from an antenna can reach an approaching aircraft through many possible paths. The first step in applying the ray-theoretic approach to the MLS problem is ray tracing, which involves the determination of all unblocked ray paths from each antenna element to the current position of the aircraft. In addition to the direct ray from the antenna to the aircraft, numerous rays will reach the aircraft after being scattered by the ground and other scatterers. A ray may undergo reflection off the surface of a scatterer, or diffraction at an edge of a scatterer. Rays emanating from an antenna may reach the aircraft after either a single reflection or diffraction or a sequence of reflections and/or diffractions, in any order. Accordingly, rays may be classified as singly reflected or diffracted rays, or higher order rays such as reflected-reflected, reflected-diffracted, diffracted-reflected-diffracted, etc. The "order" of a ray is the number of reflections and/or diffractions it undergoes before reaching the aircraft. Rays can be of infinite order, but the contribution of rays generally diminishes as their order increases (ref. 30).

For a multiwedge model, a large number of ray combinations, involving many wedges or planes, are possible, not all of which may exist in a given situation. Ray tracing to determine all possible rays

is thus a complex exercise which has conventionally been carried out by a numerical search procedure. Such a procedure requires large computational effort and yields only approximate results. In the present work, a systematic geometric method has been devised, along with the necessary computer programs, that generates exact solutions for the existence and locations of all rays up to any specified order, and tests for their existence. The geometry for testing a third-order ray is shown in figure 5.

RESULTS AND DISCUSSION

Accurate determination of the electromagnetic field at the aircraft location is an important step in the modeling. The diffraction from the edges of the wedges, as well as reflection from the plane segments of the model, is dependent on the characteristics of the scatterer, particularly its impedance. Whereas nearly all the earlier models assumed the terrain and other scatterers to be perfectly conducting, this model takes into account the impedance of the scatterers. Through an equivalence relationship, the surface roughness has also been taken into account. The ability to handle the surface undulation, surface roughness, and impedance, separately or simultaneously, makes the model both general and powerful.

The analytical/computational evaluation of the MLS thus requires the following major steps:

(1) representation of the actual airport terrain (between the elevation antenna and the aircraft position) through a multiwedge model;

(2) complete ray tracing to determine all existing rays between the antenna array and the aircraft location;

(3) estimation of the elevation angle from the computed beam envelope;

(4) repetition of steps (2) and (3) for a number of points along the flight path;

(5) comparison of the computed results with available experimental results for model validation.

Application to an Experimental Site

To demonstrate the difference in electromagnetic fields computed by using the various modeling approaches, an experimental site (ref. 7), shown in figure 6, is used for computing the fields at different elevation angles. The site has both up-slopes and down-slopes and has several features that are common in airport terrains worldwide.

The curves in figure 7 show the computed power versus elevation angle for the actual C-band measurements (ref. 32) and the results obtained by Evans et al. (ref. 7). All the curves show a similar pattern, but the one obtained using the approach outlined here follows the measured values more closely than does that of Evans. This may be due to the difference in the modeling technique and our use of accurate field estimation using impedance UTD. Also, the model developed in the present work tests for all rays of any order and combination. This means that the primary ray types (direct, reflected, and diffracted) are combined in any order up to any level, and the model automatically checks for the existence of all possible combinations for a given antenna and aircraft location. Such a scheme ensures

that the field contributions from all possible unblocked ray paths are taken into account. However, all the curves in figure 7 demonstrate the presence of direct signal at 4.2° with two prominent specular returns.

Application to a Hypothetical Airport Site

The International Civil Aviation Organization has specified (refs. 33 and 34) a flight validation process for glideslope that includes a level run and a low-level approach for measuring the vertical and structural characteristics of the glideslope. In the low-level approach, the flight is along the nominal glideslope and the error in angle should ideally remain zero throughout. In practice, however, there is generally a residual error whose prominant component is random, caused by navigational uncertainties, gusts, measurement inaccuracies, etc. The error along the nominal glideslope approach is expressed in terms of statistical parameters which are used to determine the quality of the glideslope. The error in the case of the MLS is required to be less than 0.001°.

A hypothetical airport model with the elevation antenna located at a distance 125 m from the runway center line is shown in figure 8. The desired elevation angle is 3°. The ground elevation is about 8 ft with respect to the antenna mast base. A five-plate model was used to model the terrain, and the impedance model was used for the field estimation. This permitted the inclusion of the effects of surface roughness and surface impedance, in addition to the effect of ground undulation. The surface roughness parameter is assumed to be 0.3 and the surface impedance of the dry sandy terrain is $3 - j0.06\Omega$ (per square). The computed elevation angle error for a low-level approach is shown in figure 9. The maximum error is more than 0.029°. This large error can be attributed to the up-slope in the terrain geometry considered here. Several simulations were carried out with different terrain geometries, and it was observed that only terrain undulations within 960 ft from the antenna contribute significantly to the multipath effects. Beyond 960 ft, the error is less than 0.01°. The sloping terrain within the above region is responsible for maximum error.

Application to Aircraft in the ATC Environment

The Boeing 747 aircraft, because of its large fuselage and tail fin, is expected to produce maximum error from scattering. Hence in the model, a 747 aircraft was simulated at the beginning of the runway. The error versus distance is shown in figure 10. The modeled 747 aircraft produced an error of only 0.012° for an aircraft in the final approach at a distance of about 900 ft from the instument runway. This indicates that the movement of aircraft on the runway is not likely to affect the performance of the elevation equipment. Another simulation was carried out by modeling an aircraft at a distance of 500 ft from the edge of the runway and 150 ft from the front of the elevation antenna. This resulted in an error of more than 0.025° (fig. 11), which may be unacceptable. This finding indicates that taxi tracks, roads, etc., within 500 ft from the runway and in front of the elevation antenna are likely to cause unacceptable errors.

USE OF MLS SCATTER-EFFECT MODELING IN ATC AUTOMATION

As mentioned earlier, since the MLS (unlike the ILS) is designed to provide multiple approach corridors to aircraft, errors arising from multipath effects could enhance the probability of conflict among approaching aircraft. It is therefore desirable to build MLS scatter effects into the ATC automation scheme, so that any perceptible aircraft course deviation (due to scattering) that may lead to a conflict is available as an input for the automation tool.

When the MLS model is incorporated into an automated ATC tool, the scattering environment of the MLS can be divided into two parts. One part consists of the "fixed" scatterers such as terrain features, hangars, antenna masts, and other airport structures in the MLS influence area. A map of such scatterers can be obtained, and the course aberrations due to the scatterers can be computed, for each MLS installation in the ATC network. Since such a computation can be carried out off-line, a complete and accurate analysis may be done using the impedance UTD method in conjunction with an accurate terrain model using a large number of plates or wedges. Field evaluation can be conducted at a large number of closely spaced points over the MLS coverage volume, and the vector fields at those points can be stored in computer memory as a look-up table for combination with other field contributions, such as those shown below.

The second part of the scattering environment consists of the moving (or movable) scatterers in the MLS influence volume such as parked, taxiing, or flying aircraft; parked or moving vehicles; or other temporary structures. The effects of scattering from these bodies would have to be modeled for dynamic, real-time evaluation. This requires the use of relatively simple algorithms. The process is considerably simplified by the fact that these effects need be computed only at a few discrete points that correspond to the current locations of the aircraft being guided by the MLS. It may be further simplified by assuming the scatterers to be fully conducting, an assumption that is valid for aircraft, vehicles, and metal hangars. This assumption permits the use of the simpler UTD-based field computation, which results in a several-fold savings in computational effort compared to the more elaborate impedance UTD method.

To a first order, the effect of each "temporary" scatterer may be considered separately and vectorially added to the field resulting from the fixed scatterers (retrieved from computer memory) to provide an estimate of the total aberration due to the scattering environment. The relatively weak second-order effects of the rays bouncing among the scatterers and between the scatterers and the terrain would require too much computation time for cost-effective, real-time implementation, and is not recommended at the present time.

The results of the scatterer-effect simulation would appear as an inaccuracy in position information for aircraft that utilize the MLS information for that purpose. The automated ATC system could take this error into account in its conflict detection and resolution algorithms. The criteria for separation between aircraft in each particular zone within the MLS coverage volume should be expanded to allow for the additional position inaccuracy due to scatter effects. A good criterion for combining the stipulated separation distance and the expected error due to scatter effects is to add them in a root-mean-square (rms) sense, since the actual position of the aircraft within the allocated volume and the scatter-induced errors are well-approximated as uncorrelated random variables.

Further studies in this area should include a determination, by experimental means, of the accuracy of the MLS guidance in the presence of scattering effects by comparing the position information from the MLS with that from other position location devices such as radar and the aircraft's inertial navigation system. Such an analysis will validate the accuracy of the modeling approach and pave the way for its successful integration into the ATC automation process.

CONCLUDING REMARKS

An attempt has been made in this report to present a perspective of the effects of site and other scatterers on the MLS, and to outline the developments relating to evaluation of multipath effects on the system's performance. Details of the developments and sample results were provided. It has been shown that, with a combination of modeling, ray tracing, and powerful field-evaluation techniques, it is possible to evaluate MLS multipath effects realistically.

The results of the simulations carried out in this study show that the presence of other aircraft in front of the elevation antenna induce unnacceptable errors in elevation angle. While this study has simulated sample results for terrain irregularities and scatterers like aircraft, more full-run simulations are needed to evaluate the effects in a variety of situations encountered in actual ATC operations.

The scatter-effect simulation, including the ray-tracing algorithm, is generally capable of handling any scatterer, ray order, or impedance. It can handle any airport situation, as well as other radio communication problems involving multipath effects.

The major bottleneck in the use of analytical methods for scatter-effect modeling hitherto has been the relative inaccuracy and computation-intensiveness of the methods. The MLS method is versatile enough to handle all types of scatterers encountered. This method, because of its accuracy, versatility, speed, and cost-effectiveness, is expected to make a significant contribution to ATC automation.

APPENDIX

FIELD COMPUTATION

According to GTD, the total field at an observation point is the sum of the geometric optics (GO) and diffracted fields and can be represented as (see fig. 3)

$$E^t_{s,h} = E^g_{s,h} + E^d_{s,h} = E_0 \left[\frac{e^{-jks_o}}{s_o} \mp \frac{e^{-jks''}}{s''} + \frac{e^{-jks'}}{s'} D_{s,h} e^{-jks} A_d \right] \tag{A-1}$$

where the diffraction coefficient $D_{s,h}$ and the divergence factor A_d are given by Keller (ref. 21)

$$D_{s,h} = \frac{-e^{-j\pi/4} \sin\frac{\pi}{n}}{n\sqrt{2\pi k} sin\beta_o} \left[\frac{1}{\cos\frac{\pi}{n} - \cos\frac{\beta^-}{n}} \mp \frac{1}{\cos\frac{\pi}{n} - \cos\frac{\beta^+}{n}} \right] \tag{A-2}$$

and

$$A_d = \frac{s'}{s'(s+s')} \tag{A-3}$$

Equation (A-3) is not valid in transition regions in the vicinity of shadow and reflection boundaries where it predicts infinite fields. The above drawback of the GTD has been overcome by the two uniform theories. In the UTD (ref. 22), the diffraction coefficient in equation (A-3) is modified by introducing Fresnel and cotangent functions and is given by

$$D_{s,h} = \frac{-e^{-j\pi/4}}{2n\sqrt{2\pi k}\sin\beta_o} \left[\cot\left(\frac{\pi+\beta^-}{2n}\right) F(kLa^+_-\beta^-) + \cot\left(\frac{\pi-\beta^-}{2n}\right) F(kLa^-_-\beta^-) \right.$$
$$\left. \pm \left\{ \cot\left(\frac{\pi+\beta^+}{2n}\right) F(kLa^+_+\beta^+) + \cot\left(\frac{\pi-\beta^+}{2n}\right) F(kLa^-_+\beta^+) \right\} \right] \tag{A-4}$$

where

$$F(x) = 2j \mid \sqrt{x} \mid e^{jx} \int_{|\sqrt{x}|}^{\infty} e^{-t^2} dt \tag{A-5}$$

and

$$a^{\pm}_{\pm} = 2\cos^2\left(\frac{2n\pi N^{\pm}_{\pm} - \beta^{\pm}}{2}\right) \tag{A-6}$$

$N^{\pm}_{\pm}$ = integers which most nearly satisfy the following equations:

$$2\pi n N^+_{\pm} - \beta^{\pm} = \pi \tag{A-7}$$

$$2\pi n N^-_{\pm} - \beta^{\pm} = -\pi \tag{A-8}$$

and

$$\beta^{\pm} = \phi \pm \phi' \tag{A-9}$$

The distance parameter for spherical wave incidence is given by

$$L = \frac{ss'}{s+s'} \sin^2 \beta_o \tag{A-10}$$

When the observation point moves away from the reflection and shadow boundaries, equation (A-5) is reduced to (A-3). Under this situation, the observation point is said to be outside the transition regions.

In UAT the diffracted field E^d is as in equation (A-2). The modified GO field E^{go} is given by (ref. 24).

$$E^{go} = [F(\zeta^i) - \hat{F}(\zeta^i)]E^i + [F(\zeta^r) - \hat{F}(\zeta^r)]E^r \tag{A-11}$$

where

$$F(x) = \frac{e^{-\frac{j\pi}{4}}}{\sqrt{\pi}} \int_x^\infty e^{it^2} dt \tag{A-12}$$

$$\hat{F}(x) = \frac{1}{2x\sqrt{\pi}} e^{j(x^2+\frac{\pi}{4})} \tag{A-13}$$

$$\zeta^i = \mp\sqrt{(k)} \mid (s'+s-s_o)^{\frac{1}{2}} \mid \tag{A-14}$$

and

$$\zeta^r = \mp\sqrt{(k)} \mid (s'+s-s'')^{\frac{1}{2}} \mid \tag{A-15}$$

where the positive and negative signs correspond to the shadow and lit regions respectively.

The perfectly conducting model does not take into account the surface roughness and impedance properties of the scatterer. The diffraction coefficient D_s, h in the case of impedance formulation has been shown to be (ref. 25)

$$D_{s,h} = \frac{-e^{-j\pi/4}}{n\sqrt{2\pi k}\Omega^{s,h}\phi'} \left\{ \Omega^{s,h}(\phi+\pi) \left[\cot(\frac{\pi+\beta^-}{2n}) F(kLa_-^+\beta^-) - \cot(\frac{\pi+\beta^+}{2n}) F(kLa_+^+\beta^+) \right] + \right.$$
$$\left. \Omega^{s,h}(\phi-\pi) \left[\cot(\frac{\pi-\beta^-}{2n}) F(kLa_-^-\beta^-) - \cot(\frac{\pi-\beta^+}{2n}) F(kLa_+^-\beta^+) \right] \right\}$$

where

$$\Omega^{s,h}(\alpha) = M(-\alpha+\pi/2-\theta_B^{s,h}).M(-\alpha-\pi/2+\theta_B^{s,h})$$
$$.M(-\alpha+n\pi-\pi/2+\theta_A^{s,h}).M(-\alpha+n\pi+\pi/2-\theta_A^{s,h}) \tag{A-16}$$

with the Maliuzhinets' function $M(\alpha)$ defined as (ref. 26)

$$M(\alpha) = \prod_{n'=1}^{x} \prod_{m'=1}^{x} \left[1 - (\frac{\alpha}{n\pi(2n'-1)+(\pi/2)(2m'-1)})^2 \right]^{(-1)^{m'+1}} \tag{A-17}$$

and

$$\theta_s = \sin^{-1}(\epsilon_r - \cos^2\phi')^{1/2} \tag{A-18}$$

$$\theta_h = \sin^{-1}[(\epsilon_r - \cos^2\phi')^{1/2}]\epsilon_r \tag{A-19}$$

The subscripts A and B refer to the two faces of the wedges in figure 3 and the superscripts s and h correspond to soft and hard boundary conditions on the wedge surface.

REFERENCES

1. National Plan for the Development of MLS. DOT/NASA/DOD Planning Group Report No. AD 733268, 1971.

2. Prosser, L. L., Sr.: Current Status of the MLS Program. J. Institute of Navigation, vol. 30, 1983, pp. 205-215.

3. Poulose, M. M.; Mahapatra, P. R.; and Balakrishnan, N.: Microwave Landing System- a Favoured Alternative to the Current ILS. IETE Tech. Review, vol. 2, 1985, pp. 375-382.

4. Mahapatra, P. R.; and Poulose, M. M.: Evaluating ILS and MLS sites without Flight Tests. Brit. J. Navigation, vol. 42, 1989, pp. 278-290.

5. Tobias, L.; Volckers, U.; and Erzberger, H.: Controller Evaluations of the Descent Advisor Automation Aid. NASA TM-102197, 1989.

6. Erzberger, H.; and Nedell, W.: Design of Automated System for Management of Arrival Traffic. NASA TM-102201, 1989.

7. Evans, J. E.; Capon, J.; and Shnidman, D.A.: Multipath Modeling for Simulating the Performance of the Microwave Landing System. The Lincoln Laboratory Journal, vol. 2, 1989, pp. 459-474.

8. Goodman, J. W.: Introduction to Fourier Optics. McGraw Hill Book Company, Inc., 1954.

9. Sommerfeld, A.: Optics. Academic Press, 1956.

10. Beckmann, P.: Scattering by Composite Rough Surface. Proc. IEEE, vol. 53, 1965, pp. 1012-1016.

11. Gilfillan, I. T. T.: Microwave Landing System. Phase 1 Report, Gilfillan, 1972.

12. Radio Technical Commission for Aeronautics: A New Guidance System for Approach and Landing. Report No. DO-148, 1970.

13. Sebring, J. R.; and Ruth, J. K.: MLS Scanning Beam Antenna Implementation. The Microwave Journal, vol. 1, 1974, pp. 41-46.

14. Mahapatra, P. R.; and Poulose, M. M.: A Fast and Low Cost Validation technique for ILS and MLS. IEEE Position Location and Navigation Symposium (PLANS '90), Las Vegas, Nevada, 1990.

15. Evans, J. E.; Burchsted, R. B.; Capon, J.; Orr, R. S.; Shnidman, D. A.; and Sussman, S. M.: MLS Multipath Studies. Report ATC-63, Lincoln Laboratory, 1976.

16. Morin, S.; Newsom, P.; Kahn, D.; and Jordan, L.: ILS Performance Prediction. Report FAA-RD-74-157B, Transportation System Center, Cambridge, Massachussets, 1974.

17. Ramakrishna, S.; and Sachidananda, M.: Calculating the Effect of Uneven Terrain on Glidepath Signals. IEEE Trans., vol. AES 10, 1974, pp. 380-384.

18. Cornbleet, S.: Geometrical Optics Reviewed. Proc. IEEE, vol. 71, 1983, pp. 471-529.

19. Luebbers, R.; Ungvichian, V.; and Mitchel, L.: GTD Terrain Reflection Model Applied to ILS Glideslope. IEEE Trans., vol. AES 8, 1982, pp. 11-19.

20. Poulose, M. M.; Mahapatra, P. R.; and Balakrishnan, N.: Estimation of ILS Glideslope in the Presence of Terrain Irregularities. JIETE, vol. 33, 1987, pp. 22-29.

21. Keller, J. B.: Geometrical Theory of Diffraction. J. Optical Soc. Amer., vol. 52, 1962, pp. 116-130.

22. Kouyoumjian, R. G.; and Pathak, P. H.: A Uniform Theory of Diffraction for an Edge on a Perfectly Conducting Surface. Proc. IEEE, vol. 62, 1964, pp. 1448-1461.

23. Tiberio, R.; and Kouyoumjian, R. G.: A Uniform GTD Analysis of Diffraction by Thick Edges and Strips Illuminated at Grazing Incidence. Intl. Symposium Digest, Antenna and Propagation, Univ. of Maryland, 1978.

24. Ahluwalia, D. S.; Lewis, R. M.; and Boersma, J. M.: Uniform Asymptotic Theory of Diffraction by a Plane Screen. SIAM J. Appl. Math., vol. 16, 1968, pp. 783-807.

25. Poulose, M. M.; and Mahapatra, P. R.: ILS Glideslope Evaluation for Imperfect Terrain. IEEE Trans., vol. AES 24, 1988, pp. 1886-1891.

26. Maliuzhinets: Excitation, Reflection and Emission of Surface Waves from a Wedge with Given Face Impedances. Soviet Physics Dokhladv, vol. 3, 1958, pp. 752-755.

27. Poulose, M. M.; Mahapatra, P. R.; and Balakrishnan, N.: Accurate Prediction of Terrain Undulation and Roughness Effects in Radiating Systems. Proc. IEEE Intl. Conference on Antennas and Communications, Montreal, Canada, 1986.

28. Brein, T.: Multipath Analysis of ILS Glidepath. Report N-7034, ELAB, Trondheim, Norway, 1979.

29. Poulose, M. M.; Mahapatra, P. R.; and Balakrishnan, N.: Terrain Modelling of Glideslope for Instrument Landing System. IEE Proc. Sec. H, vol. 34, 1987, pp. 275-279.

30. Poulose, M. M.; Mahapatra, P. R.; and Balakrishnan, N.: Computer Aided ILS Site Evaluation is Deemed Practical. ICAO Bulletin, vol. 48, 1986, pp. 36-39.

31. Krispin, J. W.; and Siegel, K. S.: Methods of Radar Cross-Section Analysis, Academic Press, New York, 1968.

32. Sun, D. F.: Experimental Measurements of Low Angle Ground Reflection Characteristics at L and C Bands for Irregular Terrain. Lincoln Laboratory Report ATC-107, 1982.

33. International Civil Aviation Organization: International Standards and Practices, Annexure 10, Montreal, Canada, 1968.

34. International Civil Aviation Organization: Manual on Testing of Radio Navigational Aids, Annexure 11, Montreal, Canada, 1973.

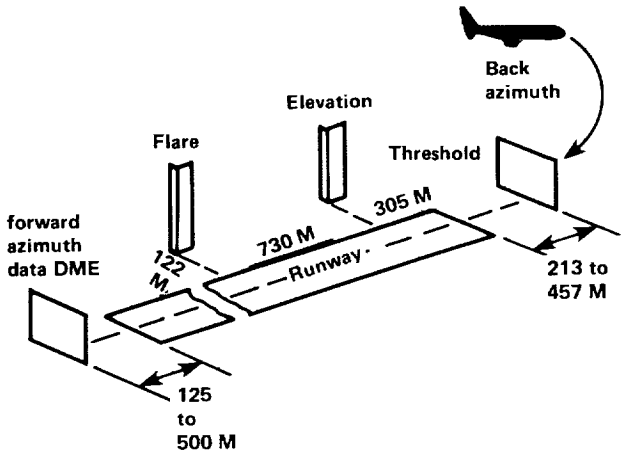

Figure 1. TRSB MLS system composition.

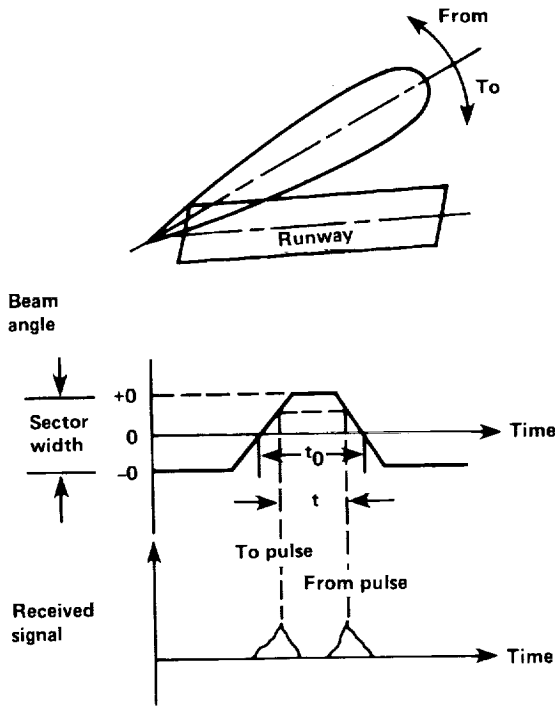

Figure 2. Beam sweep angle as a function of time.

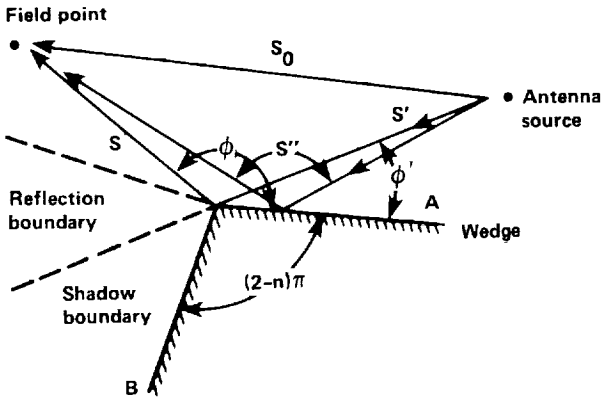

Figure 3. Wedge parameters and ray geometry.

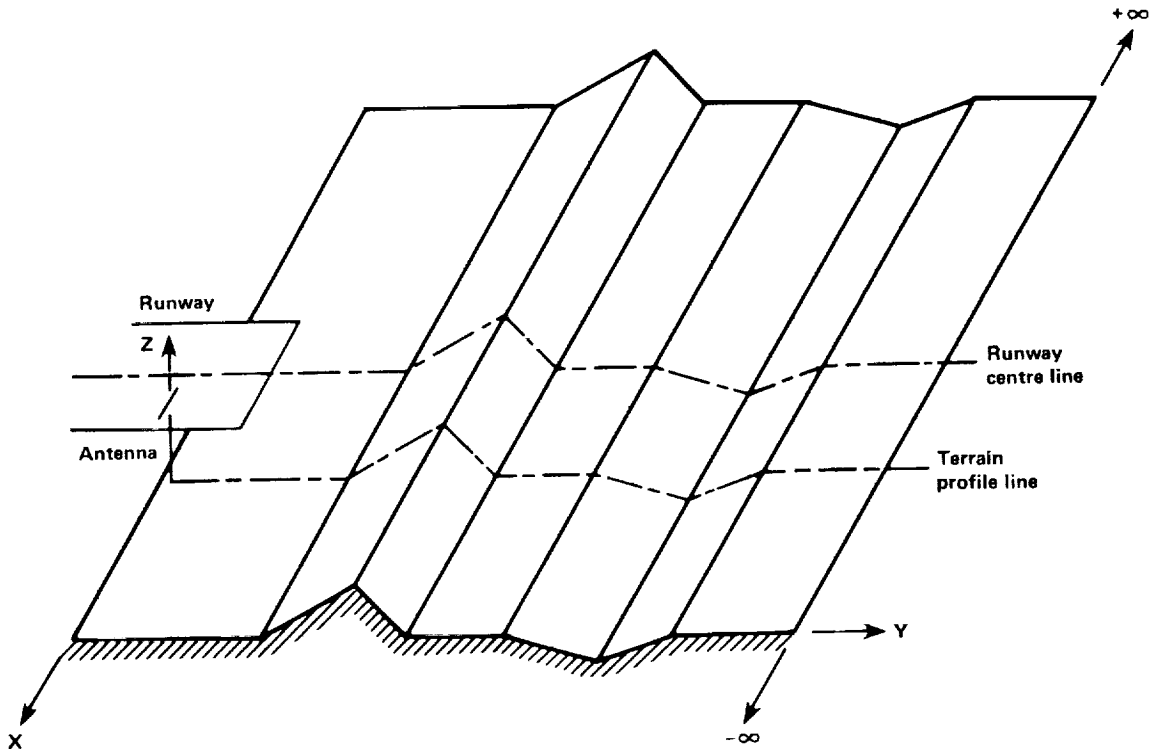

Figure 4. Schematic of a multiwedge model of an airport terrain.

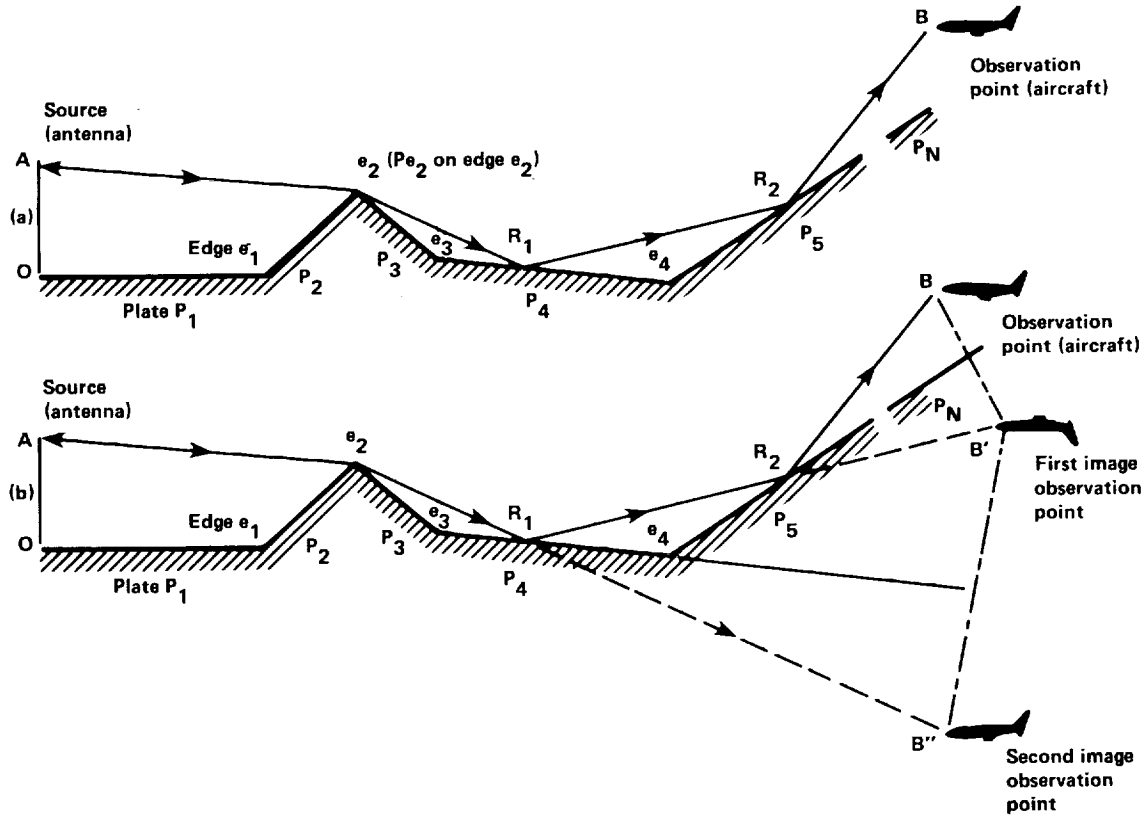

Figure 5. Geometrical basis for tracing one third-order ray. A diffracted-reflected-reflected ray is shown here as an example.

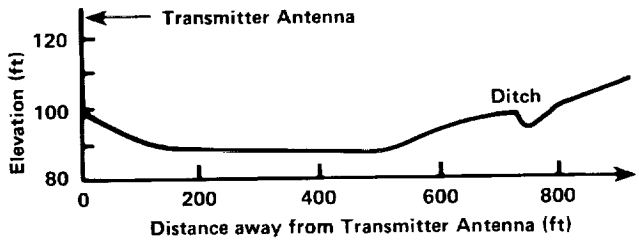

Figure 6. Experimental site (Fort Devens, Mass., Golf Course).

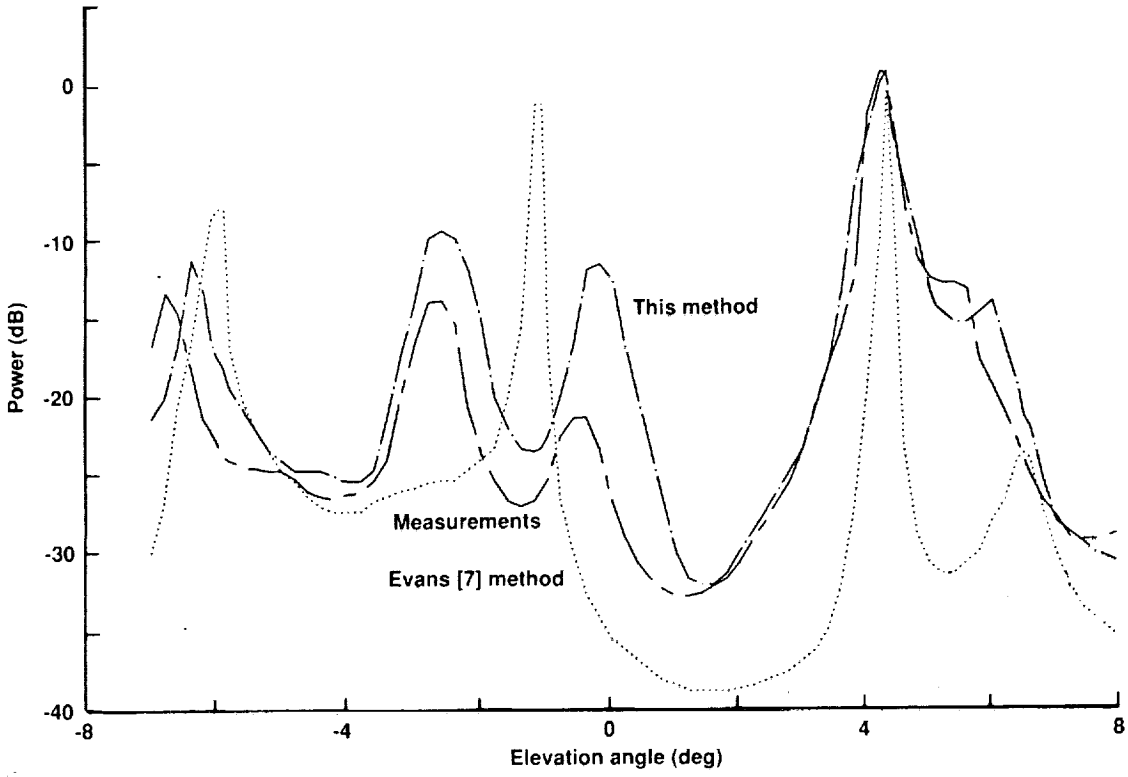

Figure 7. Computed and measured power versus elevation angle.

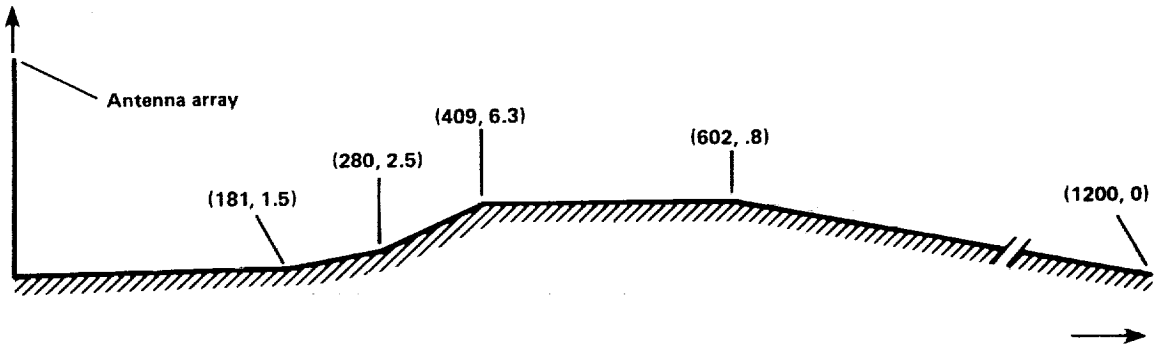

Figure 8. Five-segment approximation of a hypothetical airport site (not to scale).

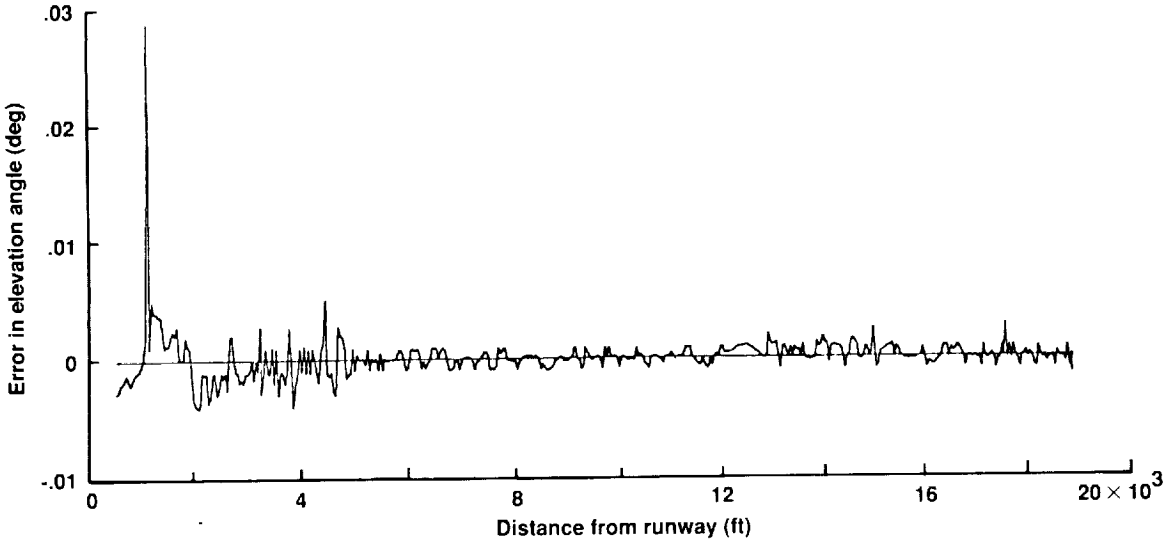

Figure 9. Computed error in elevation angle versus distance from runway for the airport site in figure 8, for a low-level approach.

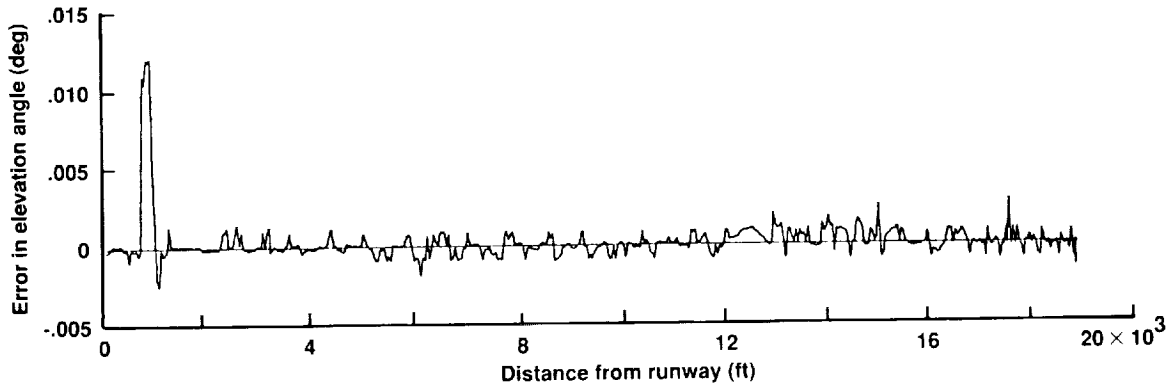

Figure 10. Computed error in elevation angle versus distance for a low-level approach when a Boeing 747 aircraft is modeled at the end of the runway.

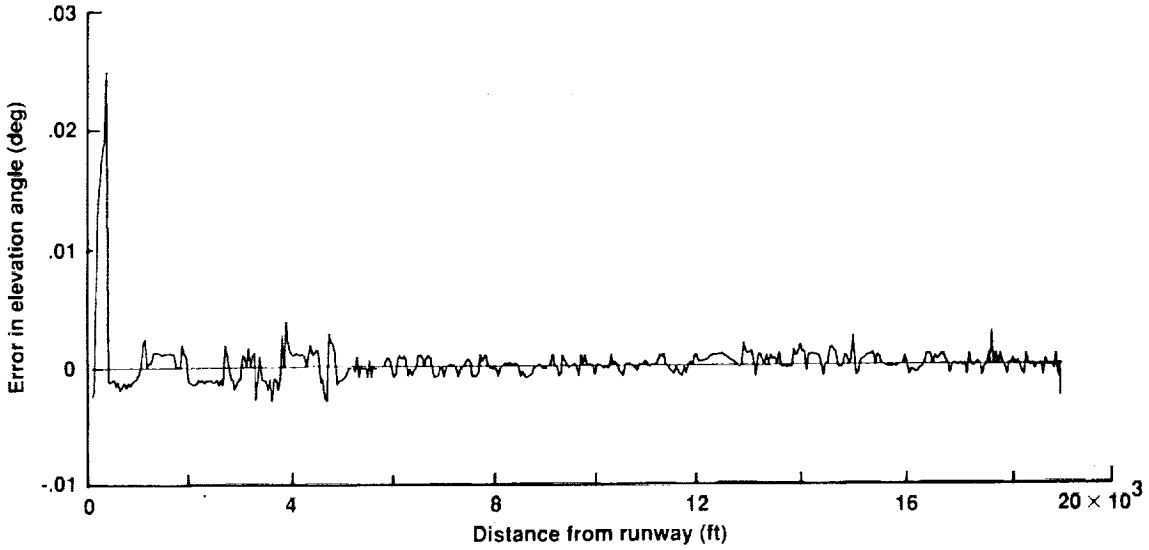

Figure 11. Computed error in elevation angle versus distance for a low-level approach when the Boeing 747 aircraft is at an offset distance of 500 ft and 150 ft to the front of elevation antenna.

NASA
National Aeronautics and Space Administration

Report Documentation Page

1. Report No.	2. Government Accession No.	3. Recipient's Catalog No.
NASA TM-102832		

4. Title and Subtitle	5. Report Date
Microwave Landing System Modeling with Application to Air Traffic Control	April 1991
	6. Performing Organization Code
7. Author(s)	8. Performing Organization Report No.
M. M. Poulose	A-90184
	10. Work Unit No.
	505-67-21
9. Performing Organization Name and Address	11. Contract or Grant No.
Ames Research Center Moffett Field, CA 94035-1000	
	13. Type of Report and Period Covered
12. Sponsoring Agency Name and Address	Technical Memorandum
National Aeronautics and Space Administration Washington, DC 20546-0001	14. Sponsoring Agency Code

15. Supplementary Notes

Point of Contact: Len Tobias, Ames Research Center, MS 210-9, Moffett Field, CA 94035-1000
(415) 604-5430 or FTS 464-5430

16. Abstract

Compared to the current instrument landing system, the microwave landing system (MLS), which is in the advanced stage of implementation, can potentially provide significant fuel and time savings as well as more flexibility in approach and landing functions. However, the expanded coverage and increased accuracy requirements of the MLS make it more susceptible to the features of the site in which it is located. This report presents an analytical approach for evaluating the multipath effects of scatterers that are commonly found in airport environments. The approach combines a multiplate model with a ray-tracing technique and a formulation for estimating the electromagnetic fields caused by the antenna array in the presence of scatterers. It can model the effects of undulation, the roughness and impedance of the terrain, and other scatterers. The model is applied to several airport scenarios. The reduced computational burden enables the scattering effects on MLS position information to be evaluated in near-real time. Evaluation in near-real time would permit the incorporation of the modeling scheme into air traffic control automation; it would adaptively delineate zones of reduced accuracy within the MLS coverage volume, and help establish safe approach and takeoff trajectories in the presence of uneven terrain and other scatterers.

17. Key Words (Suggested by Author(s))	18. Distribution Statement
Microwave landing system Air traffic control Multipath effects	Unclassified-Unlimited Subject Category - 03

19. Security Classif. (of this report)	20. Security Classif. (of this page)	21. No. of Pages	22. Price
Unclassified	Unclassified	22	A02

NASA FORM 1626 OCT 86

For sale by the National Technical Information Service, Springfield, Virginia 22161

PAGE 21 INTENTIONALLY BLANK

PRECEDING PAGE BLANK NOT FILMED